

## Newtonian and non-Newtonian flows through micro scale orifices

Shadi Ansari<sup>1</sup>, Md Ashker Ibney Rashid<sup>1</sup>, Prashant R. Waghmare<sup>2</sup>,  
Yongsheng Ma<sup>2</sup> and David Nobes<sup>2,\*</sup>

<sup>1</sup>Department of Mechanical Engineering, University of Alberta, Edmonton, Canada

<sup>2</sup>Faculty of Mechanical Engineering, University of Alberta, Edmonton, Canada

\*corresponding author: dnobes@ualberta.ca

---

**Abstract** Steam assisted gravity drainage (SAGD) is an enhanced oil recovery technology for producing bitumen and heavy crude oil. In this process, high viscosity and possibly non-Newtonian fluids flow from porous media into a production well via slots that have been machined into a production pipe. The dimensions of these narrow slots are adjusted to provide sand control and prevent solids from being produced. The SAGD process also suffers from plugging and scaling of these slotted liners. There is therefore strong interest in understanding the flow through these micro scale orifices for non-Newtonian fluids that potentially carry solids for both design of the slot for production as well as addressing failure modes. In this study, particle image velocimetry (PIV) was used to study the effect of variation in the geometry on the development of the velocity profile and subsequently the change in the upstream and downstream flow. The velocity field of Newtonian and non-Newtonian fluids through micro scale orifices is also investigated with this method. Water as a Newtonian fluid was used to generate a base case velocity field. Water mixed with 0.2 wt. % polyacrylamide was used as non-Newtonian fluid to understand the effects of changing viscosity across the flow field. For Newtonian fluid a jet was observed at the downstream of the straight micro-orifice while in the case of non-Newtonian fluid the shear thinning property of fluid suppressed the jet formation. As it was expected for the Newtonian fluid a parabolic profile was found for water and power-law velocity profile was observed for polyacrylamide solution. The obtained result from this study will be helpful for finding the optimum geometry for channels to decrease scaling and plugging of the slots in the SAGD Process.

**Keywords:** Micro-Orifice; PIV; Newtonian / non-Newtonian flow

---

### 1 Introduction

Micro-orifices have been used for various purposes such as a flow control, in choke flow meters, aircraft engine fuel supply, etc. [1-12]. Understanding velocity profiles and pressure drop across orifices are utmost priority to gain the optimum design of micro orifices. Different studies were performed to investigate and quantify the velocity profiles and pressure drop under different operating conditions. There are several parameters which can affect the velocity profile such as fluid properties, geometry and shape of the orifice and Reynolds number [1-11]. It was observed that the velocity profile is different in square and circular micro orifices and pressure drop correlation was presented for non-circular micro orifices [1-3]. The inlet and exit conditions for rectangular micro orifices were studied at high flow rate [4, 5]. In the case of experimental analysis it is difficult to perform the analysis for finding the critical value in which the flow separate in the micro orifices. Using numerical analysis it has been shown that the numerical result of 2D simulation is only consistent with 3-D results at high aspect ratio, while the 3-D numerical simulation is constant with the experimental observation in all aspect ratio [6-11]. It is evident through the numerical and experimental work performed so far [1-12] in most of the cases the operating liquid/fluid is considered as single phase and Newtonian. But in reality for numerous applications for which these studies are performed, the operating liquid is either two phase or non-Newtonian. Little attention has been given to the non-Newtonian nature of the liquid [12] and for simplicity, the orifice geometry is always considered as circular. Also, the entrance and exit effects are not studied in great detail. In this study, we investigate the importance of non-Newtonian nature of liquid and the inlet and exit parameters while quantifying the velocity profile across the micro orifice. It is to be noted that the accurate quantification of the velocity magnitude across the micro orifice is vital information for obtaining the optimum performance of the device or the process such as Steam-assisted gravity drainage (SAGD).

Steam-assisted gravity drainage (SAGD) is the enhanced oil recovery (EOR) process through which the high pressure steam is injected to obtain the optimum fluidity to the hydrocarbons (mainly bitumen in the province of Alberta, Canada) by transfer the thermal energy to the highly viscous hydrocarbons. There are

two separate wells to transport the steam and low viscous crude oil. These wells or metal bores have circumferential slots which called a slotted liner, through which the steam is ejected into the reservoir and crude oil it withdrawn. These slotted liner have rectangular cross section with 0.16-0.2 mm width [13, 14] and it can be assumed that slotted liners behave like micro orifices. In most of the cases the geometry of the slotted liners is not of uniform cross section as studied by several researchers. In this study, the velocity profile across the rectangular section micro orifice is performed and the dimensions of these micro-orifices are similar to the slotted liner used in the SAGD process. Plugging and scaling of the slotted liners on wellbore which pumps out the bitumen to surface in SAGD process is one the most important issue that needs to be resolved [15-19]. Replacing the slotted liners is not possible and cleaning is time consuming and expensive [20]. There are three different shapes for slotted liners used in the SAGD process and these are; straight, keystone and rolled; a unique geometry with a sudden expansion opening. Studying the orifice geometry and obtaining information on the velocity profile can guide slot design to obtain the optimum geometry of the slotted liners to decrease the possibility of failure [15-20].

In this paper, particle image velocimetry (PIV) was used to study the effect of variations in the geometry on the development of the velocity profile and subsequently the change in the upstream and downstream flow. Two different slotted liners - straight and keystone with dimensions typical of those found in industry was studied. It is to be noted that, in most of the cases the hydrocarbon produces in the SAGD process behaves significantly different than ideal fluid. For example the bitumen behaves as a non-Newtonian fluid at low temperature ( $< 40\text{ }^{\circ}\text{C}$ ) and Newtonian fluid at higher temperature [21]. To mimic the similar situation at lab scale a polyacrylamide / water solution with concentration of 0.2 wt. % (2000 ppm.) was used as shear thinning fluid to simulate the flow field for bitumen. Also, deionized water was used for comparison as a Newtonian fluid.

### Flow chip design

The flow cell that represents the slotted liner consists of 3 layers as depicted in Fig 1 which shows overall geometry and dimensions of the two slots investigated. The top and bottom layer are a holder and viewing window while the middle layer contains the slot of appropriate geometry. The top layer has an inlet and outlet of diameter 3.175 mm to which 1/8" tubes were connected via push to connect straight adaptors (Push-to-Connect Tube Fitting for Air and Water, Straight Adapter for 1/8" Tube OD  $\times$  10-32 UNF Male). The middle layer has a channel with straight Fig 1 (a) or keystone Fig 1 (b) orifice in the middle. The channel was designed as wide as possible to decrease the wall effect on the flow field of the orifice.

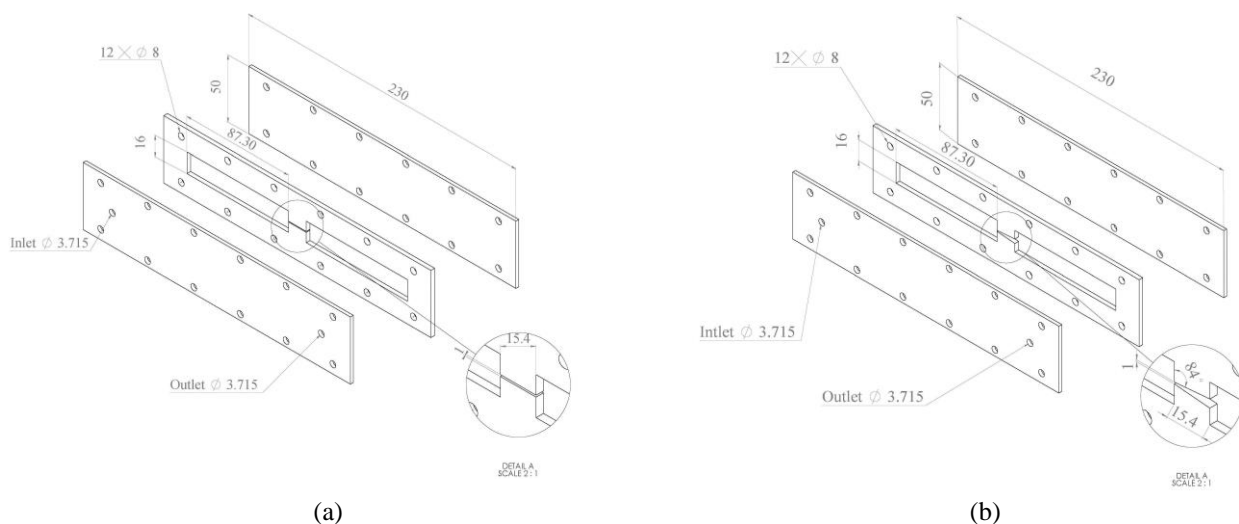


Fig. 1. Design of the flow cells for (a) the straight channel and (b) the keystone channel. All dimensions in mm.

Channels were made from sheet of PMMA (Model: Optix; Vendor: Plaskolit Inc.) and manufactured to size using a laser cutter (Model: VersaLaser VLS Version 3.50; Vendor: Universal Laser Systems). As it shown in Fig 2 an o-ring was used to seal the orifice, the top and the bottom layers. The layers were fixed together with twelve #10-24 hex socket cap head screws.

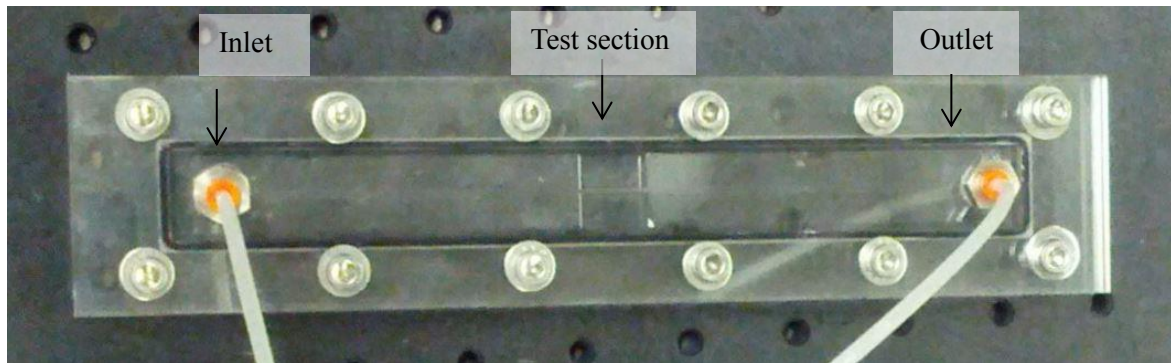


Fig. 2. Picture of chip for straight orifice

### Optical setup

An imaging setup was developed to capture the velocity field across the orifices using the arrangement shown in the schematic in Fig. 3 (a). The flow cell was mounted vertically and flow of working fluid is obtained with a specific gravity head. To avoid any gas bubble in the flow cell, the working fluid was pumped from bottom to top to make sure the channel was completely filled with liquid only. A camera (Model: SP-5000M-PMCL-CX; Vendor: Jai Inc) with resolution of  $2560 \times 2048$  pixels was used to capture series of images with defined time sequence. A 50mm lens with  $f\# = 4$  (NIKKOR 50mm, Nikon) was used to capture the entire orifice in the field of view. To freeze the particle motion a high current green  $4'' \times 4''$  side-fired LED back light (BX0404-520 nm; Advanced Illumination Inc.) was used as a light source in pulsed mode with the control of a strobe controller (Pulsar 320 Strobe Controller; Advanced Illumination Inc.) to generate  $5\mu\text{sec}$  flashes of light. The LED and Camera were synchronized and controlled by a function generator (TDS 2024B; Tektronix Inc.). At the very low Reynold number of the flow the capturing rate was set to 20fps. To trace the fluid hollow glass microspheres (ASTM C169; Potters Industries Inc) made of fused borosilicate glass with mean diameter of  $18\mu\text{m}$  and bulk density of  $0.49 \text{ g.cm}^{-3}$  were added to the solutions as seeding particles. the images capture formed a shadowgraph of the particle position. The complete setup of the entire experimental setup is shown in the digital image in Fig. 3(b).

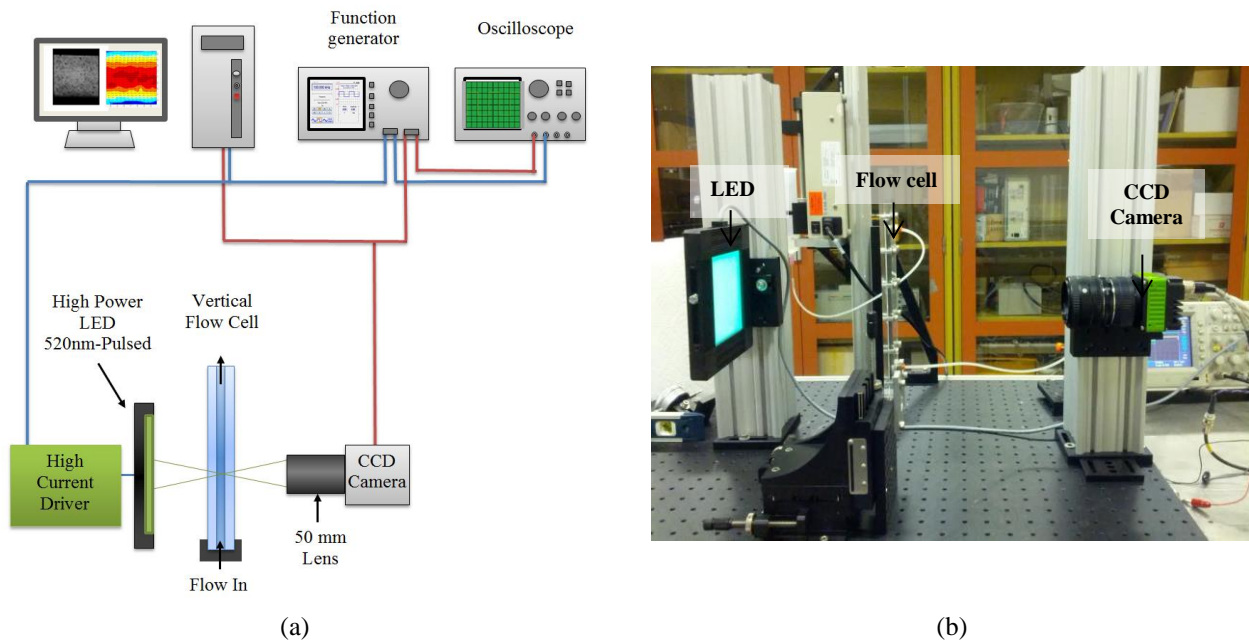


Fig. 3. Optical used for capturing the velocity profile(a) Schematic of optical setup and (b) picture of optical setup

## Solution and seeding

Deionized water (DI) water was used as the Newtonian fluid and 0.2 wt. % polyacrylamide was added to form a solution that was used as the non-Newtonian fluid. To prepare polyacrylamide solution, a commercial sample of high molecular weight anionic polyacrylamide powder was used (BASF SE Germany). The solution was prepared using the standard method reported in the literature [22]. The viscosity of polyacrylamide solution was measured using a rheometer [RheolabQC; Anton Paar] with a double gap cylinder measuring system (DG42). The variation of viscosity of polyacrylamide solution with respect to the change in the shear rate is shown in Fig. 4 (a). As observed in the literature the viscosity decreases by increasing the shear rate which reflects that the fluid (0.2 wt. % polyacrylamide in water) is a shear thinning fluid and the dominance of shear-thinning behavior decreases by increasing the shear rate. The flow index of this fluid was obtained from the shear stress response as presented in Fig. 4 (b) for non-Newtonian fluid the relation between shear rate and viscosity is shown in equation 1

$$\tau = \tau_0 + K\gamma^n \quad (1)$$

where  $\tau$  is the shear stress,  $\gamma$  is shear rate,  $\tau_0$  is yield stress and  $K$  is the regarded factor and  $n$  is flow index. For 0.2 wt. % polyacrylamide in water as shown in Fig. 4 and using the Herschel–Buckley fluid model, for this fluid the flow index was  $n = 0.5384$ , yield stress was  $\tau_0 = 1.5495$ , and  $K = 0.27834$ .

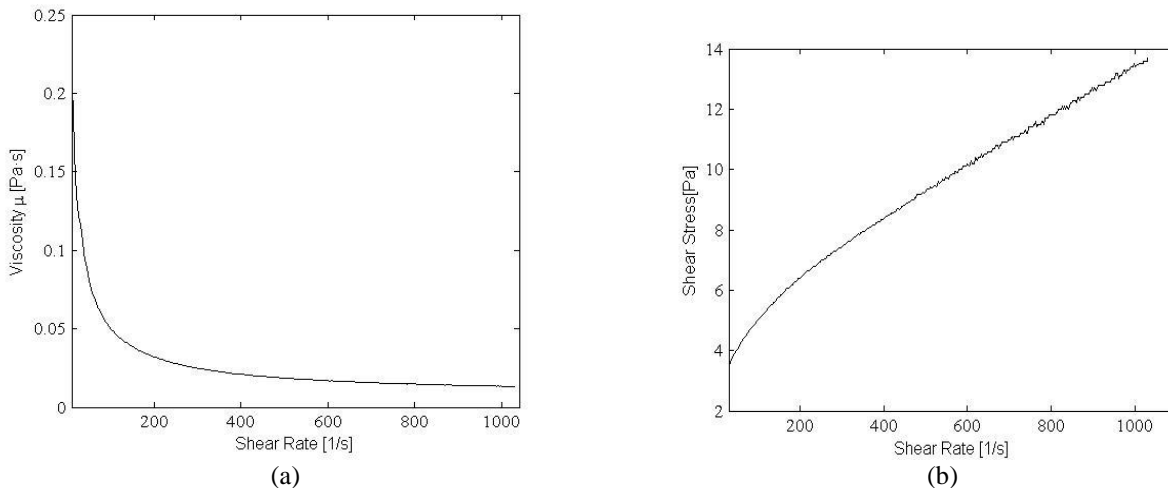


Fig. 4. Rheological measurement of non-Newtonian fluid (0.2 wt. % polyacrylamide solution) for obtaining the velocity profile information showing (a) the variation in viscosity with the change in the shear rate and (b) the variation in the stress with respect to the shear rate. The resolution for shear rate was 1/5 s.

## PIV Processing

The ultimate goal of this study was the analyses the velocity profiles across the micro-orifice. An example data image from the sequence of images of the flow passing through the specially designed micro-orifice is as shown in Fig. 5(a). Captured images were inverted using the commercially available image processing software (DaVis Imaging Software 8.1.4, LaVision GmbH.) and a geometric mask was applied to decrease the noises for processing. Both raw image and the inverted image with mask are shown in Fig. 5 (a) and (b), respectively. Decreasing multi-pass time series cross correlation was applied for identifying the displacement vector magnitude and direction. The particles sizes are around 1 to 2 pixels with displacement of around 4 to 5 pixels between sequential images. A window size of the first pass was 96×96 and the window size of the second pass was 32×32, both of an 87% overlap. The final velocity profile was obtained by averaging over 200 consecutive images.

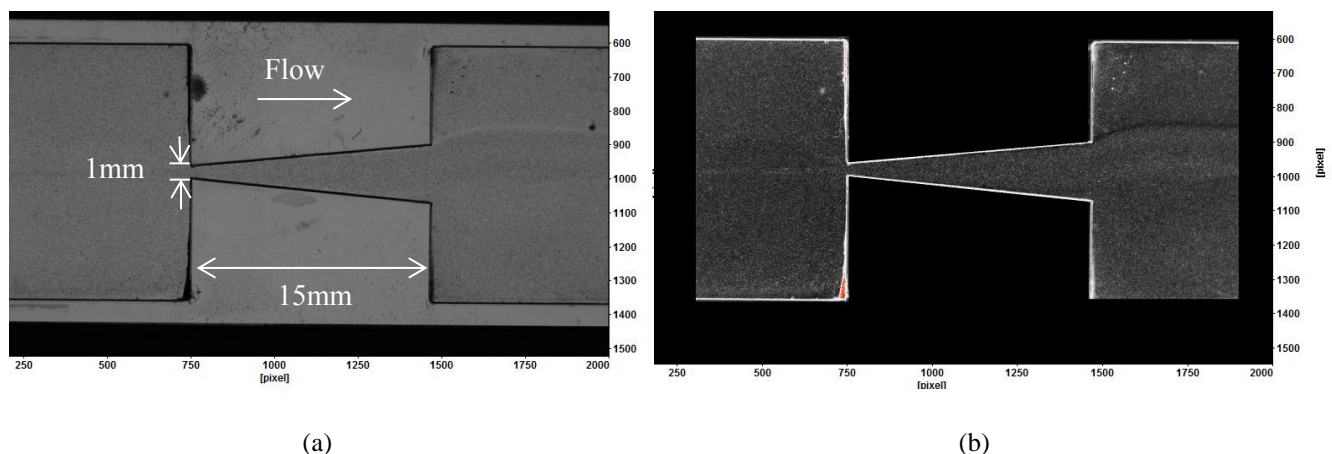
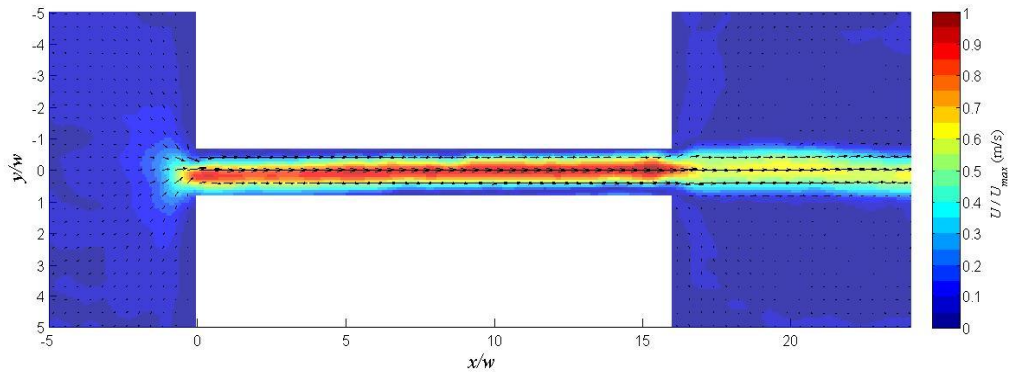


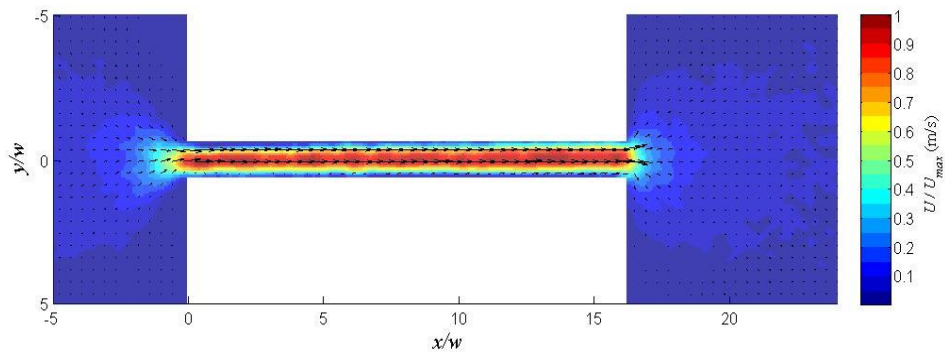
Fig. 5. Images of keystone channel used for PIV analysis (a) raw image and (b) inverted PIV image with geometric mask

## Velocity profile along the channel

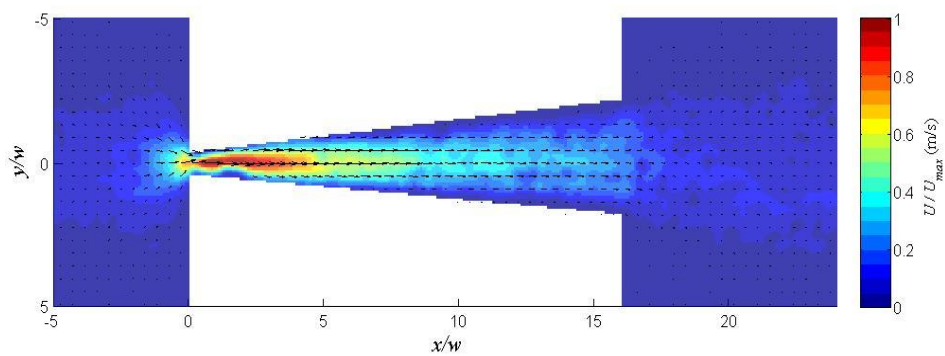
The variation in the development of the flow (i.e, the development of the velocity profile across the channel along the direction of the flow) was studied for different geometry to analyze the effect of the channel shape on the developing velocity profile. Fig. 6 depicts the two different cases where the geometry of the micro-orifice is changed from uniform cross section (straight) to non-uniform cross section (keystone) along the direction of the flow. A velocity vector map showing every 5<sup>th</sup> vector with a scaled background colour map of velocity magnitude shows the general flow characteristics. The velocity background was normalized based on the maximum velocity in the channel and the length of the channel was normalized based on the width of the entrance. In Fig. 6(a) and (b) the fluid at  $Re \approx 5$  is captured. It is evident that in this case of the Newtonian fluid the momentum in the fluid results in a jet formation at the exit of the channel. The length at which this momentum disappears is one of the interesting and unanswered questions which needs further attention. For the case of the non-Newtonian fluid, at the exit, for the same  $Re$ /flow rate, the fluid experiences a sudden expansion instantaneously at the exit. The shear thinning nature of liquid retards the liquid motion significantly at the exit; therefore the jet formation as observed with Newtonian fluid was not observed here. As it is shown in Figs. 6 (b) and (c), in the case of keystone expansion where the width of the channel increases along the flow direction the jet formation was not observed in either case. The change in the shape of the micro-orifice dominates the rheology of the liquid. In this case, the exit effects are same, irrespective of the nature of liquid (Newtonian or non-Newtonian). The outcome due the change in the liquid rheology and change in the geometric configuration can be further analyzed by investigating the development of the velocity profile across both micro-orifices.



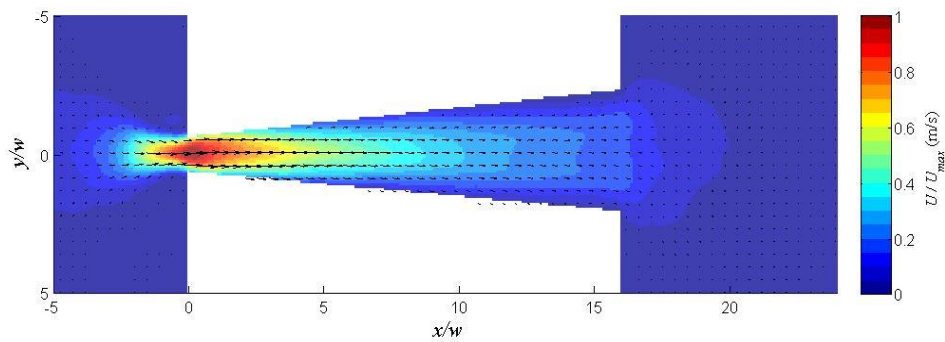
(a)



(b)



(c)



(d)

Fig. 6. Average velocity vector map (only every 5<sup>th</sup> vector shown) with a background colour map of velocity magnitude for (a) water through straight channel, (b) 0.2 wt. % polyacrylamide through straight channel, (c) water through keystone channel and (d) 0.2 wt. % polyacrylamide through keystone channel

Profiles of velocity for the Newtonian and non-Newtonian fluid along the length of the micro-orifices were studied and compared for straight and keystone channel in Figs. 7 (a) to (d). Figures 7(a) and (b) show the development of normalized velocity profile with Newtonian and non-Newtonian fluid along the uniform cross-section micro-orifices. The location  $x/w = 0$  represents the entrance of the micro-orifice and  $x/w = 16$  is the exit of the micro-orifice. In the case of the Newtonian fluid in a straight channel, Fig. 7(a) the expected parabolic velocity profile was observed with a gradual change in the centerline velocity. In the case of the non-Newtonian fluid, Fig. 7(b), the change in the centerline velocity was similar to the Newtonian fluid.

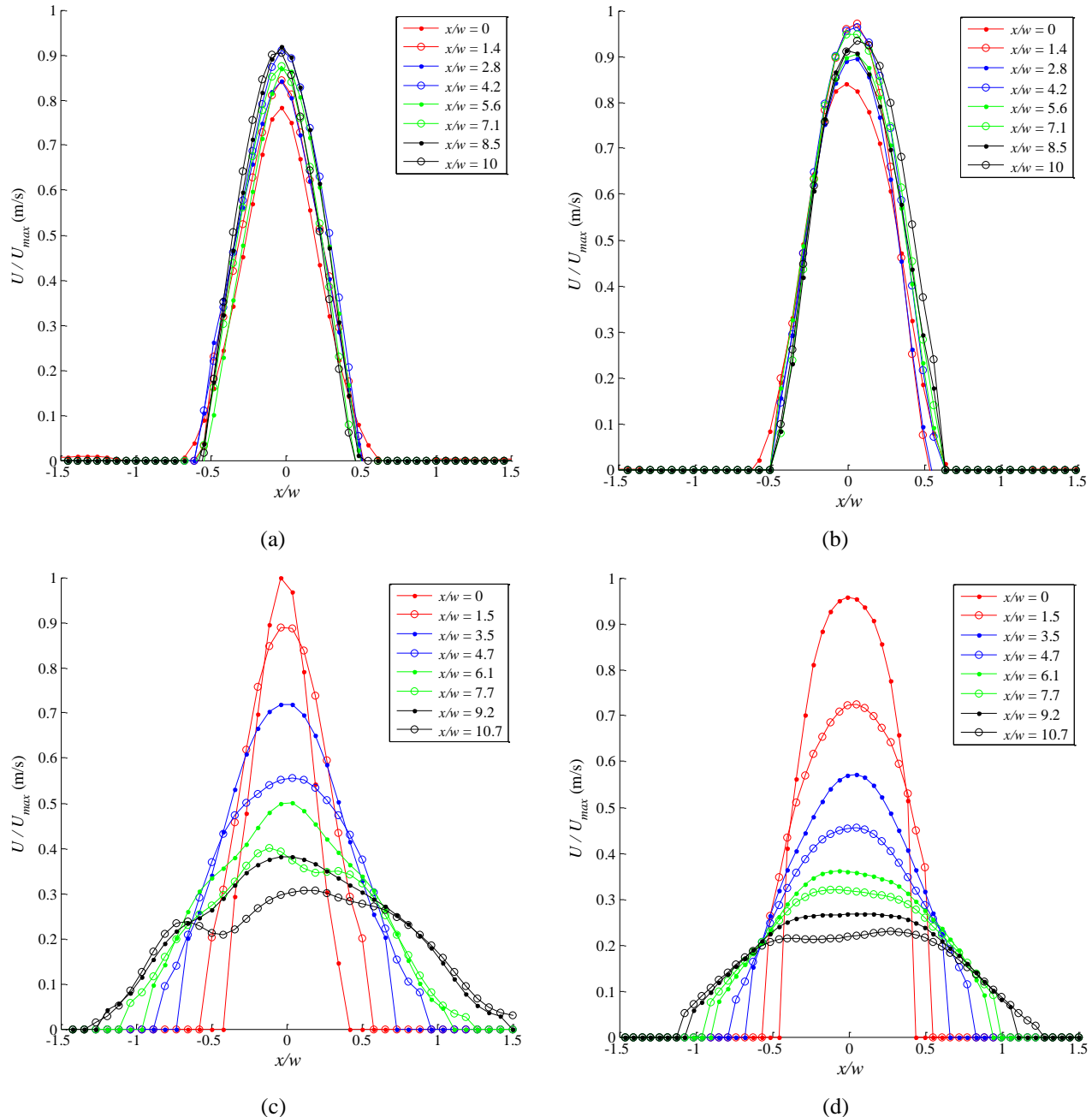


Fig. 7. Velocity profile of (a) water through straight channel, (b) 0.2 wt.% polyacrylamide through straight channel, (c) water through keystone channel and (d) 0.2 wt.% polyacrylamide through keystone channel

In order to find the effect of geometry on the velocity profile the development of the normalized velocity profile across the keystone channel was also studied and the results are shown in Fig 7(c) and (d). Figure 7(c) shows the development of velocity profile for Newtonian fluid, in this case the velocity has parabolic profile at the entrance of the orifice and it remains the same up to  $x/w = 3.5$ . In the case of non-Newtonian fluid also, Fig. 7(d), it remains parabolic. Beyond this length, the velocity profile was significantly different for Newtonian and non-Newtonian fluids. In the case of non-Newtonian fluid the velocity profile in the middle of the channels flattens and attains the profile similar to plug-like velocity profile. The centerline velocity of

both Newtonian and non-Newtonian fluid through keystone channel decreases toward the downstream. Another interesting aspect was the fluctuations in the velocity profile near the wall region. The sudden change in the channel dimension generates the fluctuations near the wall regions; in the case of non-Newtonian fluid the fluctuations are dampened to shear thickening nature of the fluid.

## Conclusion

In this study, the effect of the fluid properties and geometric variations in the micro-orifice on the average velocity field were studied for Newtonian as well non-Newtonian fluid. The velocity profile across two types of micro-orifices, straight and keystone channel, was observed. The velocity profile was obtained using a shadowgraph PIV method. Water and 0.2 wt. % polyacrylamide were used as Newtonian and non-Newtonian fluid. For the Newtonian fluid a jet was observed at the downstream of the straight micro-orifice while in the case of non-Newtonian fluid the shear thinning property of fluid suppressed the jet formation. As it was expected for the Newtonian fluid, parabolic profile was found for water and power-law velocity profile was observed for polyacrylamide solution. In the case of keystone channel with non-uniform cross section along the direction of the flow, the centerline velocity profile of the Newtonian and non-Newtonian fluid shows similar behavior. The obtained result from this study will be helpful for finding the optimum geometry for channel to decrease scaling and plugging of them in SAGD Process.

## Acknowledgements

The authors gratefully acknowledge financial support from Natural Sciences and Engineering Research Council (NSERC) of Canada, the Alberta Ingenuity Fund, and the Canadian Foundation for Innovation (CFI).

## References

- [1] Xu, B., Ooi, K. T., & Wong, N. T. (2000). Experimental investigation of flow friction for liquid flow in microchannels *Int. Commun. Heat Mass Transfer*, 27(8), 1165–1176.
- [2] Sousa, P. C., Coelho, P. M., Oliveira, M. S. N., & Alves, M. a. (2009). Three-dimensional flow of Newtonian and Boger fluids in square–square contractions. *Journal of Non-Newtonian Fluid Mechanics*, 160(2-3), 122–139. <http://doi.org/10.1016/j.jnnfm.2009.03.009>
- [3] Sousa, P. C., Coelho, P. M., Oliveira, M. S. N., & Alves, M. a. (2011a). Effect of the contraction ratio upon viscoelastic fluid flow in three-dimensional square–square contractions. *Chemical Engineering Science*, 66(5), 998–1009.
- [4] Tsukahara, T., Motozawa, M., Tsurumi, D., & Kawaguchi, Y. (2013). PIV and DNS analyses of viscoelastic turbulent flows behind a rectangular orifice. *International Journal of Heat and Fluid Flow*, 41, 66–79
- [5] Afonso, a. M., Oliveira, P. J., Pinho, F. T., & Alves, M. a. (2011). Dynamics of high-Deborah-number entry flows: a numerical study. *Journal of Fluid Mechanics*, 677, 272–304.
- [6] Oliveira, M. S. N., Rodd, L. E., McKinley, G. H., & Alves, M. a. (2008). Simulations of extensional flow in microrheometric devices. *Microfluidics and Nanofluidics*, 5(6), 809–826. <http://doi.org/10.1007/s10404-008-0277-5>
- [7] Walters, K., Webster, M. F., & Tamaddon-Jahromi, H. R. (2009). The numerical simulation of some contraction flows of highly elastic liquids and their impact on the relevance of the Couette correction in extensional rheology. *Chemical Engineering Science*, 64(22), 4632–4639.
- [8] Chowdhury, M. R., & Fester, V. G. (2012). Modeling pressure losses for Newtonian and non-Newtonian laminar and turbulent flow in long square edged orifices. *Chemical Engineering Research and Design*, 90(7), 863–869. <http://doi.org/10.1016/j.cherd.2011.11.001>

- [9] Mishra, C., & Peles, Y. (2005). Flow visualization of cavitating flows through a rectangular slot micro-orifice ingrained in a microchannel. *Physics of Fluids*, 17(11), 113602. <http://doi.org/10.1063/1.2132289>
- [10] Mishra, C., & Peles, Y. (2005). Size scale effects on cavitating flows through microorifices entrenched in rectangular microchannels. *Journal of Microelectromechanical Systems*, 14(5), 987–999. <http://doi.org/10.1109/JMEMS.2005.851800>
- [11] Tsai, C.-H., Chen, H.-T., Wang, Y.-N., Lin, C.-H., & Fu, L.-M. (2006). Capabilities and limitations of 2-dimensional and 3-dimensional numerical methods in modeling the fluid flow in sudden expansion microchannels. *Microfluidics and Nanofluidics*, 3(1), 13–18.
- [12] Muzychka, Y. S., & Edge, J. (2008). Laminar Non-Newtonian Fluid Flow in Noncircular Ducts and Microchannels. *Journal of Fluids Engineering*, 130(11), 111201.
- [13] Bennion, D. B., Gupta, S., Gittins, S., Corporation, E., & Hollies, D. (2009). Protocols for Slotted Liner Design for Optimum SAGD Operation. *Canadian Petroleum Technology*, 48, 21–26.
- [14] Kumar, A., Srivastava, A. K., & Kumar, R. (2013). Design Optimization of Slotted Liner Completions in Horizontal Wells of Mumbai High Field. *SPE Asia Pacific Oil and Gas Conference and Exhibition*.
- [15] Dall'Acqua, D., Lopez Turconi, G., Monterrubio, I., Allen, M.D. (2007). Development of an Optimized Tubular Material for Thermal Slotted Liner Completions PS Canadian International Petroleum Conference, Calgary, Alberta, Canada, June 12–14, 2007. CIPC Paper 2007–142.
- [16] Cheung, T., Scheck, M., & Limited, S. C. (2013). SPE 164048 Novel Scale Remediation for Steam Assisted Gravity Drainage ( SAGD ) Operations, SPE International Symposium on Oilfield Chemistry, April 8-10, 2013
- [17] Kaiser, T. M. V., Wilson, S., & Venning, L. A. (2002, December 1). Inflow Analysis and Optimization of Slotted Liners. Society of Petroleum Engineers. doi:10.2118/80145-PA
- [18] Romanova, U. G., & Ma, T. (2013). An Investigation on the Plugging Mechanisms in a Slotted Liner from the Steam Assisted Gravity Operations. *SPE European Formation Damage Conference & Exhibition*. <http://doi.org/10.2118/165111-MS>
- [19] Sousa, P. C., Coelho, P. M., Oliveira, M. S. N., & Alves, M. a. (2011b). Laminar flow in three-dimensional square–square expansions. *Journal of Non-Newtonian Fluid Mechanics*, 166(17-18), 1033–1048. <http://doi.org/10.1016/j.jnnfm.2011.06.002>
- [20] Lalchan, C., Wiggins, C. & Moriyama, C. (2011). CSUG / SPE 146709PP Formulation of an Emulsified Thermal Acid Blend for SAGD Applications in Eastern Alberta, Canadian Unconventional Resources Conference, Calgary, Alberta, Canada, 15–17 November 2011.
- [21] Zhao, Y., & Machel, H. G. (2012). Viscosity and other rheological properties of bitumen from the Upper Devonian Grosmont reservoir, Alberta, Canada. *AAPG Bulletin*, 96(1), 133–153.
- [22] Zhang, L., Dong, J., Jiang, B., Sun, Y., Zhang, F., & Hao, L. (2015). A study of mixing performance of polyacrylamide solutions in a new-type static mixer combination. *Chemical Engineering and Processing: Process Intensification*, 88, 19–28.